agriculture

Article

Analysis of Interactions among Greenhouse Gas Emissions, Carbon Sinks, and Food Security in China's Agricultural Systems

Wenjie Yang * and Xiaoyun Mo

College of Mathematics and Statistics, Hunan University of Finance and Economics, Changsha 410205, China; moxyun72@163.com
* Correspondence: yangweijie@hufe.edu.cn or gs_ywj@163.com

Abstract: Reducing greenhouse gas (GHG) emissions and increasing the size of carbon sinks are closely related to food security in agricultural systems. This study conducted an in-depth data analysis of previous studies to explore the dynamic causal relationships among the reduction of emissions, carbon sink increases, and food security in agricultural systems. The fixed-effect regression model, causality tests, PVAR model, impulse response functions, and variance decomposition were used to explore correlations among the three variables. The results show that the national average carbon sinks surged from 2662.194 Mg in 2000 to 4010.613 Mg in 2020, with the food security index concurrently climbing from 0.198 to 0.308. Moreover, GHG emissions exhibited a negative growth rate from 2016 onwards, yet the 2020 mean remained 142.625 Mg above the 2000 baseline. The agricultural "three subsidies" reform has not directly promoted food security, but significantly inhibited GHG emissions. However, conflicts exist between emissions reduction and carbon sinks increase in agricultural systems and food security. At the whole level, changes in carbon sinks only have a positive effect on the increase in GHG emissions, whereas changes in GHG emissions have a positive effect on both carbon sinks and food security. Changes in food security strongly inhibit the increase in carbon sinks. This relationship varies among distinct grain functional zones. Policy objectives should be coordinated, target thresholds set, and policies classified according to different functional orientations, to achieve a win–win situation for food supply and low-carbon development.

Keywords: GHG emissions; carbon sinks; food security; panel vector autoregression model; agricultural system

check for updates

Citation: Yang, W.; Mo, X. Analysis of Interactions among Greenhouse Gas Emissions, Carbon Sinks, and Food Security in China's Agricultural Systems. *Agriculture* **2024**, *14*, 703. https://doi.org/10.3390/agriculture14050703

Academic Editor: Lijun Liu

Received: 18 March 2024
Revised: 27 April 2024
Accepted: 28 April 2024
Published: 29 April 2024

1. Introduction

Amid the impacts of global climate change, the pandemic, and geopolitical conflicts, food security has again become a pressing concern [1–3]. The 2022 report *The State of Food Security and Nutrition in the World* highlighted that, in 2021, 29.3% of the global population faced moderate to severe food insecurity, representing an increase of 350 million people since the outbreak. China has recorded 19 years of increased grain production and is therefore prioritizing food security. However, agriculture and food production accounted for 31% of the global anthropogenic greenhouse gas (GHG) emissions in 2019, with China's agricultural GHG emissions ranking the highest globally, accounting for 14% of the total emissions [4]. Among the three agricultural sources, the proportion of GHG emissions from agricultural production activity is consistently higher than that from livestock [5].

Agriculture, a major contributor to carbon sources and sinks, is the most vulnerable sector affected by climate change [6,7]; therefore, it is an integral part of climate change mitigation [8]. However, implementing mitigation programs in the agricultural sector may limit food availability and sustainable rural livelihoods in the coming decades [9–11]. For instance, implementing agricultural emission reductions in densely populated countries, such as China, may result in significant food heat loss but may not significantly contribute to emission reduction. However, increasing carbon sinks in agricultural soil can mitigate implicit heat loss [8]. A previous study has demonstrated that the increase in atmospheric CO_2 concentration enhances the carbon sink capacity of terrestrial ecosystems while causing global warming through the greenhouse effect [12]. However, the "fertilization effect" displayed by CO_2 has different or even opposing effects on yields for different countries and food crops [13]. Furthermore, the nutritional quality of food crops deteriorates when the CO_2 concentration reaches a certain level [14], potentially leading to severe public health problems [15]. The agricultural system is a significant carbon pool. It has been estimated that China's farmland has a total carbon pool of 16.32 ± 0.41 Pg C, with the soil carbon pool accounting for >96% of the total carbon pool [16]. Increasing soil carbon sinks can improve the soil quality and crop yield [17]. However, excessive fertilization can reduce the soil absorption of CH_4 and N_2O [18]. High CO_2 concentrations can increase the net primary productivity of terrestrial ecosystems [19,20], i.e., the "fertilization effect" of CO_2, which has increased global annual photosynthesis by 11.85%, equivalent to approximately 13.98 Pg C per year [21]. However, this fertilization effect is limited [22], since as the CO_2 concentration continues to increase, the effect on plant growth promotion will weaken [23]. These findings indicate that conflicts and synergies between food security and agricultural dual-carbon goals exist, with trade-offs in the short term. Despite this, in the long term, ecological security largely controls sustainable food security [24,25].

To achieve reductions in emissions and an increase in sinks while ensuring food security, a comprehensive balance is required [26,27]. Previous studies have reported correlations between agricultural production and carbon emissions [28,29]; however, the correlations among the three variables have not been investigated, which could lead to a deviation from the dual-carbon goals of agriculture and food security. Therefore, determining the correlations among GHG emissions, carbon sink capacity, and food security is necessary to achieve sustainable agricultural development.

This study aimed to explore the correlations among emissions reduction, carbon sinks increase, and food security in agricultural systems using China as a case study, analyze the differences in the correlations, and propose different implementation paths based on functional positioning differences of main grain production areas (PA), balance areas (BA), and main consumption areas (CA) in the three regions. For this purpose, a fixed-effect regression model, a causality test, panel vector autoregression (PVAR) model, impulse response function, and variance decomposition were used to examine the correlations and mechanisms affecting agricultural systems.

2. Materials and Methods

2.1. Variable Definition

2.1.1. Calculation of GHG Emissions from Agricultural Systems

The agricultural system provides a critical foundation for ensuring food security and has significant effects on GHG emissions [30]. Reducing emissions and increasing carbon sinks in farmland play crucial roles in mitigating climate change [17]. There are three primary sources of GHG emissions from farmland. First, crop planting and the use of agricultural inputs, such as fertilizers, pesticides, plastic films, machinery, and irrigation, all contribute to CO_2 emissions during the planting process. The second source is that of CH_4 emissions produced during crop growth, as paddy fields are major sources of CH_4 due to anaerobic fermentation during long-term flooding [31]. The warming potential of 1 kg CH_4 is 25 times that of 1 kg CO_2 over 100 years [32]. However, CH_4 emissions from dryland crops are negligible. Therefore, this study mainly focused on the emission of CH_4 from paddy fields. CH_4 emissions vary regionally due to climate, temperature, and other factors [33,34]. In Chinese provinces, the coefficient already includes the effect of fertilization on CH_4 emissions from paddy fields, including early rice, late rice, and in-season rice. The third source is that of N_2O emissions from farmland soils. Due to external N input, N_2O emissions from agricultural sources account for ~60% [35], and the warming potential of 1 kg N_2O is 298 times that of 1 kg CO_2 over 100 years [32] and its greenhouse effect cannot be ignored. Nitrogen fertilizer application and crop uptake have the most prominent effect on N [36].

This work refers to nitrous oxide emission factors provided by [33] to calculate soil background N_2O emissions and N_2O emissions caused by fertilization. As statistical data only provide the total amount of fertilizer application, the proportion of different crop planting areas and amount of fertilizer applied to crops were calculated in this study.

GHG emissions (10^4 Mg) were calculated based on the warming potential of three GHGs:

$$\begin{aligned} GHG &= f_{CO_2} + f_{CH_4} \times 25 + f_{N_2O} \times 298 \\ &= \sum_{i=1}^{l} C_i \times \delta_i + \sum_{j=1}^{m} H_j \times \sigma_j \times 10^{-7} \times 25 + \sum_{k=1}^{n} (S_k \times \alpha_k + N_k \times \beta_k + F_k \times \gamma_k) \times 298 \end{aligned} \quad (1)$$

where f_{CO_2}, f_{CH_4}, and f_{N_2O} denote farmland carbon, CH_4, and N_2O emissions (10^4 Mg), respectively; i, j and k denote the type of carbon, CH_4, and N_2O emissions source, respectively; C_i (10^4 Mg) is the amount of the carbon emission source; δ_i is the emission factor of the carbon emission source; H_j (hm^2) is the sown area of paddy fields; σ_j (kg/hm^2) is the emission factor of CH_4 emissions; S_k (hm^2) is the sown area of crops; N_k (10^4 Mg) is the amount of nitrogen fertilizer applied to crops; F_k (10^4 Mg) is the amount of compound fertilizer applied to crops; α_k (kg/hm^2) is the emission coefficient of crop cultivation; β_k (kg/kg) is the emission coefficient of nitrogen fertilizer; γ_k (kg/kg) is the emission coefficient of compound fertilizer.

2.1.2. Calculation of Carbon Sinks in Agricultural Systems

The amount of carbon sinks (*sink*) in agricultural systems includes the amount of CO_2 absorbed by the aboveground part of the crops and the carbon content of the underground part. It can be calculated by referring to [37]:

$$sink = \frac{CP \times (1-\delta) \cdot C_A}{C_e} \times (1+r) \quad (2)$$

where CP represents the crop yield in 10^4 Mg; δ is the water content of the crop yield as a percentage [38]; C_A represents the carbon sinks rate as a percentage; C_e indicates the economic coefficient of the crop, which is the ratio between crop output and economic output [39]; r is the ratio of the carbon content in the underground part of the crop to the carbon content of the aboveground part. Specific parameters were defined by [40].

2.1.3. Calculation of Food Security Index

Based on the perspective of ensuring grain production security and protecting productive farmland, a comprehensive evaluation of China's provincial grain security was conducted in this study from three aspects: per capita grain availability, grain yield per unit area, and cultivated land pressure. Per capita grain availability and grain output per unit area are important indicators for measuring food security, whereas the cultivated land pressure index reflects the relationship between grain production and demand [41,42] and is widely used in regional food security assessments. The equation for calculating the food security index (*food*) is:

$$food = \sum_{i=1}^{n} F_i \omega_i \quad (3)$$

$$F_k = S_{\min}/S_a = \beta \frac{G_r}{p \cdot q \cdot k \cdot S_a} \quad (4)$$

where F_i represents the i-th food security sub-indicator, $n = 3$; ω_i is the weight of the sub-indicator, calculated according to the entropy method; F_k is the cultivated land pressure index; $S_{\min}$ (hm^2) is the minimum per capita cultivated land area; β is the grain self-sufficiency rate; G_r is the per capita grain demand; p represents the grain yield per unit area; q is the ratio of the grain sown area to the total sown area; k is the multiple cropping index; and S_a (hm^2) is the actual per capita cultivated land area. National-level data were used in this study due to the lack of provincial-level data on the per capita grain demand and grain self-sufficiency rate. The G_r value is 437 kg, representing the goal of achieving an all-round well-off society in 2020, as put forward by the National Food and Nutrition Advisory Committee. According to the white book on China's grain problem (Information Office of the State Council of the People's Republic of China 1996) and 2008 Outline of the National Food Security Medium and Long-term Plan, the baseline grain self-sufficiency rate in China is 95%, therefore the value of β was calculated according to this.

2.1.4. Agricultural Policy Dummy Variable

During the study period, China implemented two crucial policies pertaining to food security and agricultural emission reduction: the grain direct subsidy policy and the agricultural "three subsidies" reform. To assess the impact of these policies on agricultural emissions reduction, carbon sinks, and food security, we established two dummy variables specific to agricultural policies. The first dummy variable, designated as fsp, represents the grain direct subsidy policy. This policy was initially piloted in major grain-producing regions in 2002; a value of 1 was assigned to these regions and 0 to others. Since its nationwide rollout in 2004, the fsp has maintained a value of 1 in all subsequent years. The second dummy variable, tsp, corresponds to the agricultural "three subsidies" reform policy. In 2015, China embarked on a fertilizer "zero growth" initiative in five provinces: Anhui, Shandong, Hunan, Sichuan, and Zhejiang, to pilot the reform, which merged various agricultural subsidies into a unified agricultural support and protection subsidy. Therefore, the tsp variable was assigned a value of 1 for the pilot provinces in 2015 and 0 for other regions. Subsequently, in 2016, the reform was expanded nationwide, resulting in a value of 1 for the tsp in all subsequent years. The objective of this policy is to encourage farmers to adopt comprehensive measures, such as straw recycling, soil loosening, reduced usage of chemical fertilizers and pesticides, and increased application of organic fertilizers.

2.1.5. Control Variables

Based on the available data and relevant literature [5,6,30] on the factors that influence food security and agricultural carbon emissions, we identified three types of influencing factors as control variables: first, population factors, including population density and population urbanization rate; second, economic factors, including Engel's coefficient, agricultural industry structure, agricultural economic development level, and agricultural mechanization level; and finally, climatic factors, including precipitation and agricultural disaster rate.

The definitions of the variables are presented in Table 1. To effectively prevent potential errors arising from extreme values during regression, we selected the logarithm of certain variables, particularly in cases where the variables have a wide range of variation.

Table 1. Statistical description of variables.

Variable	Definition	Obs.	Mean	Std.	Min	Max
CO_2	Carbon dioxide emissions (10^4 Mg)	651	253.996	193.427	3.467	870.981
CH_4	Methane emissions (10^4 Mg)	651	30.498	42.650	0.000	145.773
N_2O	Nitrous oxide emissions (10^4 Mg)	651	1.513	1.277	0.012	5.566
sink	Carbon sinks (10^4 Mg)	651	3411.399	3000.900	46.837	12,537.790
GHG	Greenhouse gas emissions (10^4 Mg)	651	1467.379	1296.201	8.599	4438.733
food	Food security index	651	0.256	0.119	0.068	0.874
fsp	Food subsidy policy (Yes = 1, no = 0)	651	0.849	0.358	0.000	1.000
tsp	Agricultural "three subsidies" reform (Yes = 1, no = 0)	651	0.246	0.431	0.000	1.000
pop	Population density (Person/hm^2)	651	4.262	6.276	0.021	39.492
szl	Disaster-affected rate	651	0.228	0.161	0.000	0.936
stru	Value added of the primary industry/GDP	651	0.120	0.065	0.003	0.364
lnmac	Logarithm of total power of agricultural machinery	651	7.431	1.104	4.543	9.499
urban	Urbanization rate of population	651	0.488	0.181	0.131	0.896
lnae	Logarithm of agricultural output value/population	651	7.672	0.697	6.147	9.454
ec	Engel's coefficient	651	0.347	0.051	0.197	0.490
rain	Logarithm of precipitation	651	6.722	0.513	4.954	7.711

2.2. Research Methods

2.2.1. Baseline Regression Model

We used a fixed-effect regression model for baseline regression. The basic model is expressed as follows:

$$Y = \lambda + cX + \sum_{j=1}^{n} \eta_j C_j + v_i + \delta_t + \varepsilon_{it} \tag{5}$$

where i is the individual, representing different regions; t is the time, representing different years; X constitutes any two of the following three variables: greenhouse gas emissions, carbon sinks, and food security; c is the core explanatory variable's estimated coefficient; C_j is the control variable j; n is the number of control variables; v_i and δ_t denote the provincial fixed effect and time fixed effect, respectively; and ε_{it} is the random disturbance item.

2.2.2. Panel-VAR Model

The PVAR model combines the advantages of the panel data model and the VAR model, hence treating all variables in the system as endogenous [43,44], and contains short time measurement estimated using the generalized method of moments (GMM) process [45]. Moreover, the orthogonalized impulse response function (IRF) of the model provides a convenient means to articulate the dynamic interplay among variables [46]. To comprehensively investigate the correlation among GHG emissions, carbon sinks, and food security in agricultural systems, the PVAR estimation method was employed in this study to construct the panel autoregressive model:

$$y_{it} = \beta_0 + \sum_{j=1}^{k} \beta_j y_{i,k-j} + \alpha_i + \eta_t + \varepsilon_{it} \tag{6}$$

where i is the individual, representing different regions; t is the time, representing different years; y_{it} is the $m \times 1$ vector of individual observable random variables i at time t; β_0 is the intercept items vector; β_j is the $m \times m$ coefficient of the lag variable matrix; $y_{i,k-j}$ is the j order lag item of endogenous variables; α_i is the individual fixed effect item; η_t is the time effect item; and ε_{it} is the random disturbance item.

2.3. Data Source

In this study, we utilized panel data from 31 provinces in China (excluding Hong Kong, Macau, and Taiwan) from 2000 to 2020. Primary data sources for this study include the National Bureau of Statistics (https://data.stats.gov.cn), the China Rural Statistical Yearbook, and Provincial Statistical Yearbook. The precipitation data are sourced from the Daily Dataset of China's Ground-based Climatic Data (V3.0) provided by the National Meteorological Science Data Sharing Service Platform.

3. Results

3.1. The Trend and Correlation between GHGs, Carbon Sinks, and Food Security

3.1.1. GHGs, Carbon Sinks, and Food Security Trends

Figure 1 illustrates the change rates of the GHG emissions, carbon sinks, and food security index in China from 2001 to 2020. Except for several years, including 2003, 2009, and 2016, both food security and carbon sinks demonstrate a growth trend. In 2003, China experienced its largest decline in grain output of 5.77% due to accelerated agricultural structural adjustments in the early 20th century, urban expansion taking up considerable areas of cultivated land, and a severe natural disaster. Subsequently, in 2004, the Central Committee of the Communist Party of China introduced a series of policies, such as direct subsidies for grain, improved seed subsidies, and agricultural tax reductions and exemptions, which augmented farmers' income and increased their willingness to cultivate grain. In 2009, China's grain output continued to grow, and the sown area increased further, resulting in a 3.54% decrease in the grain output per unit area and, ultimately, a decline in the food security index. Similarly, the food security index dropped in 2016 due to the decline in per capita grain production. GHG emissions demonstrated a growth rate of 5.50% in 2004 and did not display a downward trend until 2016. Following the Ministry of Agriculture and Rural Affairs of China's implementation of the zero-growth campaign for chemical fertilizers and pesticides in 2015, their use in the entire country has shown a steady decrease. Therefore, the warming potential has exhibited negative growth since 2016.

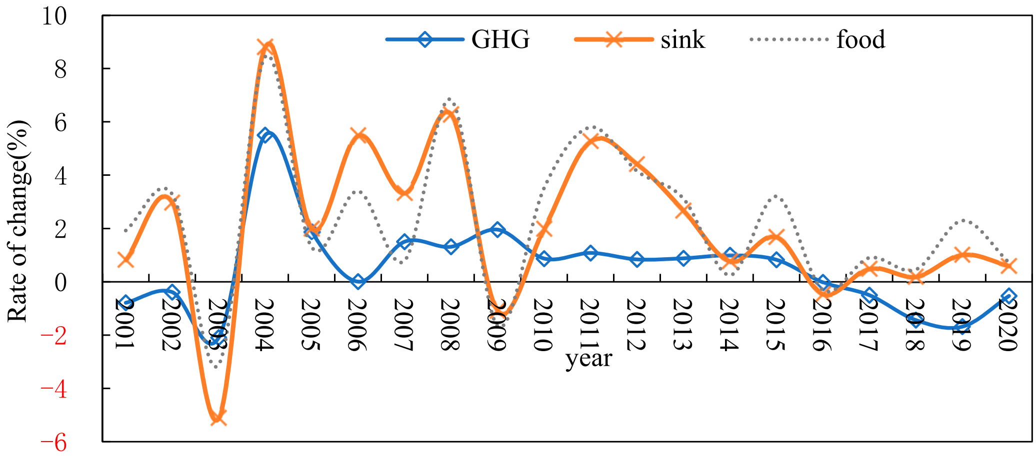

Figure 1. Change rates of GHGs, carbon sinks, and food security.

The spatiotemporal differences of GHGs, carbon sinks, and food security were analyzed by region using 2000 and 2020 as examples (Table 2). Based on the division of grain functional areas, the food security and carbon sink capacity of PA have significantly improved from 2000 to 2020, but the GHG of this area has also slightly increased. Heilongjiang had the highest food security capacity in the country in 2020, but its warming potential is at a medium level. Major rice-producing areas in the Yangtze River Basin, such as Hunan, Jiangsu, and Anhui, have high GHG emissions but low-carbon sinks and food security maintenance capabilities. Agricultural systems in Hebei, Jiangsu, Shandong, and Sichuan exhibit reduced emissions, increased sinks, and improved food security capacities. The highest number of carbon sinks was obtained for Henan. The change trend of BA and PA is consistent, but the gap between PA and BA's GHG and the average value is widening, whereas the gap in carbon sinks is narrowing. Guangxi maintains high GHG emissions and a high carbon sink capacity, ranking second in the country, but with a relatively weak ability to guarantee food security. Tibet, Qinghai, and Ningxia's GHG and sink rankings have remained stable, whereas Ningxia's food security index has significantly improved. Shanxi, Guangxi, and Chongqing have realized reduced emissions, increased sinks, and improved food security in agricultural systems. The food security index of Xinjiang is the highest in BA but still lower than the PA mean. Although the GHG emission mean has decreased in the main grain sales area, it remains higher than that in the BA area. The carbon sinks have also declined. Beijing's GHG emissions, carbon sinks, and food security index are at low levels, whereas Guangdong has the highest GHG emissions and carbon sinks in CA, but its food ranks third from the bottom and has declined. Tianjin is the only region in CA that has achieved GHG emissions reduction, carbon sinks increase, and food security index growth.

Table 2. Spatiotemporal distribution of GHGs, carbon sinks, and food security in 2000 and 2020.

Area	GHG (10^4 Mg)		Sink (10^4 Mg)		Food	
	2000	**2020**	**2000**	**2020**	**2000**	**2020**
Hebei	1465	1261	4451	6435	0.187	0.322
Inner Mongolia	533	1107	2081	6350	0.193	0.614
Liaoning	722	772	1676	3745	0.165	0.365
Jilin	751	989	2534	5998	0.283	0.690
Heilongjiang	1351	2534	4067	11,515	0.257	0.874
Jiangsu	4188	4138	4934	5662	0.292	0.342
Anhui	3387	4104	4143	6430	0.207	0.351
Jiangxi	2887	3868	2456	3108	0.239	0.304
Shandong	2119	1800	7077	9527	0.266	0.358
Henan	2077	2560	7574	12,178	0.239	0.396
Hubei	3176	4093	3749	4406	0.260	0.309
Hunan	3554	4408	4056	4457	0.276	0.322
Sichuan	2279	2243	5015	5445	0.246	0.280
PA mean	**2192**	**2606**	**4140**	**6558**	**0.239**	**0.425**
Shanxi	428	425	1252	2138	0.106	0.231
Guangxi	2404	2208	5982	11,704	0.189	0.203
Chongqing	827	826	1493	1494	0.201	0.245
Guizhou	768	884	1782	1539	0.164	0.159
Yunnan	669	1013	3868	4914	0.166	0.229
Tibet	9	15	67	47	0.230	0.238
Shaanxi	678	774	1726	2052	0.125	0.192
Gansu	300	449	1095	1859	0.107	0.254
Qinghai	26	31	130	166	0.068	0.124
Ningxia	105	145	376	569	0.186	0.314
Xinjiang	377	852	2528	6479	0.270	0.404
BA mean	**599**	**693**	**1845**	**2997**	**0.165**	**0.236**
Beijing	103	26	243	50	0.141	0.165
Tianjin	113	76	215	362	0.101	0.239
Shanghai	325	182	268	124	0.229	0.258
Zhejiang	1941	1186	1802	930	0.217	0.198
Fujian	1456	990	1201	703	0.187	0.203
Guangdong	2725	2278	3984	3607	0.200	0.185
Hainan	393	321	703	336	0.146	0.183
CA mean	**1008**	**723**	**1202**	**873**	**0.174**	**0.204**
ALL mean	**1359.226**	**1501.871**	**2662.194**	**4010.613**	**0.198**	**0.308**

Notes: Color gradient legend displayed by column across three distinct regions. PA is the main grain production areas. BA is the balance areas. CA is the main consumption areas. Food represents food security index. min max.

3.1.2. Emissions and Trends of Three GHGs

Figure 2 displays the emissions and change rates of the three GHGs, which were converted into the warming potential. CH_4 emissions from the cropland system contribute the most to the warming potential, whereas CO_2, which has the highest concentration among the main GHGs, contributes the least. Therefore, CH_4 and N_2O emissions should be considered in evaluations of the greenhouse effect caused by the cropland system, rather than just CO_2 emissions. From 2000 to 2003, methane emissions decreased annually, whereas CO_2 and N_2O emissions maintained a growth trend. This is related to the reduction of the grain crop area and increase in the economic crop area during the same period. After the implementation of the grain protection policy in 2004, CH_4 emissions increased rapidly to 229.07 million t. In 2016, the growth rates of the three GHGs significantly decreased, with CO_2 and N_2O having notable emission reduction effects. However, the reductions of the three GHGs were smaller in 2019.

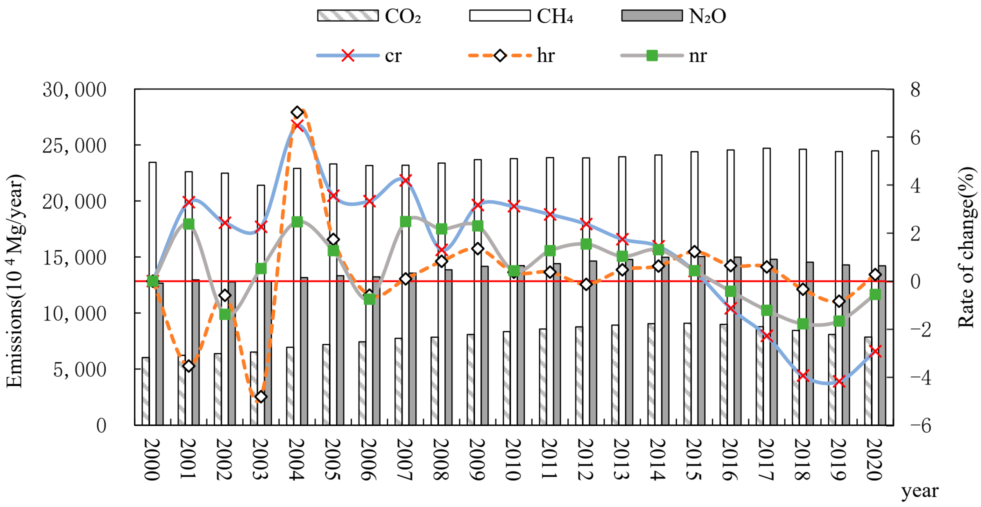

Figure 2. Emissions and change rates of CO_2, CH_4, and N_2O. Cr, hr, and nr represent the change rates of CO_2, CH_4, and N_2O, respectively.

3.1.3. Correlation Analysis of GHGs, Carbon Sinks, and Food Security

As a whole, there is a high correlation between GHGs, carbon sinks, and food security (Figure 3). The correlation coefficient between carbon sinks and GHGs is 0.772 (Table 3), which indicates a relatively strong positive correlation between carbon sinks and GHGs. The result suggests an association between the capacity of ecosystems to absorb GHGs and the emissions of these gases; however, a more in-depth investigation and data analysis remain warranted to determine the specific mechanisms. Among the three GHGs, CO_2 shows the highest correlation with food, whereas N_2O exhibits the strongest correlation with carbon sinks.

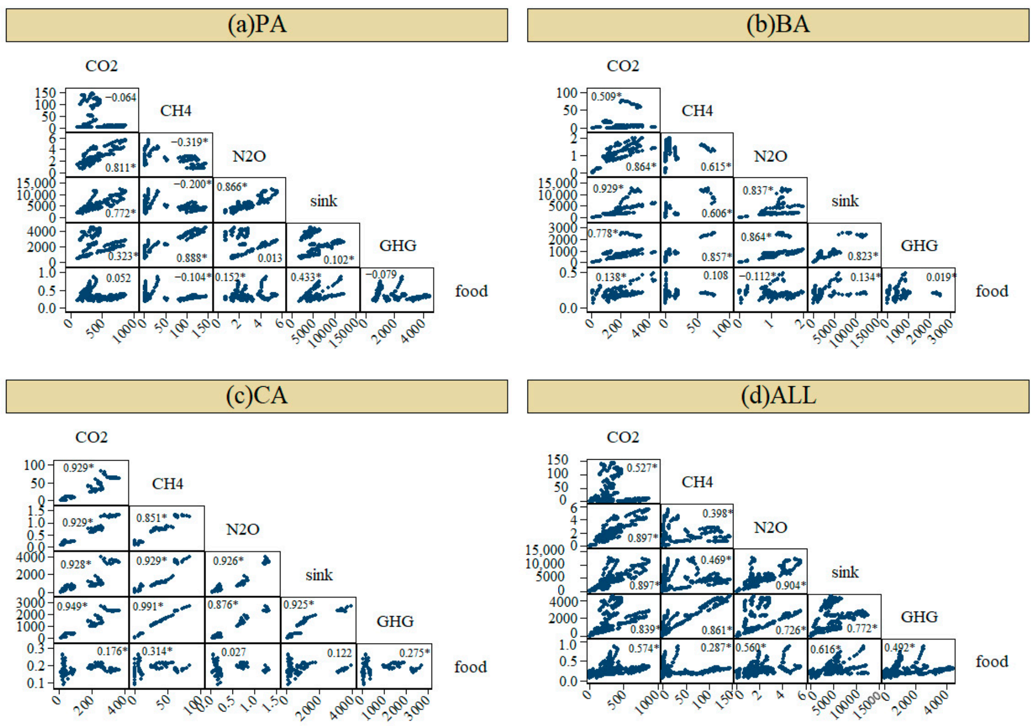

Figure 3. Scatterplot Matrix. The data in the figure represent the Spearman correlation coefficient. (**a**) Main grain production areas. (**b**) Balance areas. (**c**) Main consumption areas. (**d**) All areas. * significant at the 10% level.

Table 3. Spearman correlation coefficient.

Areas	Variables	CO_2	CH_4	N_2O	Sink	GHG	Areas	CO_2	CH_4	N_2O	Sink	GHG
PA	CH_4	−0.064					BA	0.509 *				
	N_2O	0.811 *	−0.319 *					0.864 *	0.615 *			
	sink	0.772 *	−0.200 *	0.866 *				0.929 *	0.606 *	0.837 *		
	GHG	0.323 *	0.888 *	0.013	0.102 *			0.778 *	0.857 *	0.864 *	0.823 *	
	food	0.052	−0.104 *	0.152 *	0.433 *	−0.079		0.138 *	0.108	−0.112 *	0.134 *	0.019 *
CA	CH_4	0.929 *					ALL	0.527 *				
	N_2O	0.929 *	0.851 *					0.897 *	0.398 *			
	sink	0.928 *	0.929 *	0.926 *				0.897 *	0.469 *	0.904 *		
	GHG	0.949 *	0.991 *	0.876 *	0.925 *			0.839 *	0.861 *	0.726 *	0.772 *	
	food	0.176 *	0.314 *	0.027	0.122	0.275 *		0.574 *	0.287 *	0.560 *	0.616 *	0.492 *

Notes: The data in the figure represent the Spearman correlation coefficient. PA is the main grain production areas. BA is the balance areas. CA is the main consumption areas. ALL represents all areas. * significant at the 10% level.

However, significant regional differences were observed in the correlations between variables. Sink and GHG are highly correlated in all three regions, but the correlation is the strongest in CA, with a coefficient of 0.925 (Table 3). This illustrates the dual nature of agriculture as a carbon source and sink, with the highest correlation between the two observed in CA. This is associated with the land-use patterns in these regions, where the land use in CA is more specialized and centralized. This specialization may lead to larger-scale agricultural activities and corresponding GHG emissions while providing more opportunities to implement carbon sink measures. Sink and food are significantly correlated only in PA and BA and the correlation is the strongest in PA, which might be attributed to effective land-use practices or agricultural policies promoting both carbon sinks and food production. GHG and food are only significantly correlated in BA and CA, but the correlation is weak. In terms of the correlations between the three GHGs and food, CO_2 and food only correlate in BA and CA and do not significantly correlate in PA. In PA, CH_4 and food are significantly negatively correlated, whereas they are positively correlated in BA and CA. N_2O and food are positively correlated in PA, negatively correlated in BA, and not significantly correlated in CA, suggesting that local food security is not directly related to the GHG warming potential and CO_2 emissions, although the main grain-producing regions contribute the most to whole GHG emissions and play a critical role in ensuring food security.

3.2. Analysis of Fixed Effects Regression Results

Fixed effects regression can control unobserved factors that do not change over time but vary among different units, thus more accurately estimating the relationship between variables. Through fixed effects regression, whether there are significant statistical relationships between agricultural GHG emissions, carbon sinks, and food security, as well as the direction and strength of these relationships, can be determined, thereby providing a foundation and basis for subsequent deeper causal analysis. To identify the impact of agricultural policy implementation on these three factors, we included a policy dummy variable in the model. Additionally, considering the lagged effect of policy implementation, we included a lagged policy dummy variable. Furthermore, we incorporated the interaction term between individual effects and time effects.

Result in columns (1), (3), and (5) of Table 4 show the regression results without controlling for time-fixed effects, while columns (2), (4), and (6) control for these fixed effects. From the regression results that control for all fixed effects, the growth of GHG emissions promotes the growth of carbon sinks, and vice versa, which may be related to the fertilization effect of CO_2 [19,21]. GHG emissions have an inhibitory effect on food security; however, the combined effect of GHG emissions and carbon sinks can promote food security, meaning that the impact of GHG emissions on food security may vary depending on changes in carbon sinks.

Table 4. Regression results.

Variable	(1) lnsink	(2) lnsink	(3) lnGHG	(4) lnGHG	(5) lnfood	(6) lnfood
lnsink			0.381 ***	0.361 ***	−0.197	−0.117
			(3.901)	(3.810)	(−1.608)	(−0.899)
lnfood	0.276	0.352	0.052	0.063		
	(0.531)	(0.627)	(0.143)	(0.179)		
lnGHG	0.829 ***	0.813 ***			−0.751 ***	−0.559 ***
	(4.194)	(3.608)			(−5.530)	(−3.732)
c.lnfood×c.lnGHG	0.058	0.045				
	(0.764)	(0.572)				
c.lnfood×c.lnsink			−0.021	−0.011		
			(−0.518)	(−0.281)		
c.lnsink×c.lnGHG					0.105 ***	0.084 ***
					(7.055)	(4.661)
fsp	−0.009	−0.038	−0.019	0.006	0.022	0.001
	(−0.557)	(−1.286)	(−1.276)	(0.213)	(1.322)	(0.022)
L.fsp	−0.041	−0.057 **	0.029 **	0.027	0.035 **	−0.003
	(−1.648)	(−2.161)	(2.053)	(1.378)	(2.358)	(−0.126)
tsp	−0.019	0.042	0.036 *	−0.053 ***	0.015	−0.028
	(−0.722)	(1.442)	(1.897)	(−3.122)	(0.696)	(−1.195)
L.tsp	0.010	0.048	−0.037 ***	−0.071 ***	0.002	−0.024
	(0.653)	(1.215)	(−3.957)	(−2.839)	(0.144)	(−0.941)
pop	0.004	0.007	−0.018 *	0.000	0.001	−0.021 ***
	(0.592)	(0.323)	(−1.985)	(0.015)	(0.213)	(−2.800)
szl	0.015	0.012	0.057 *	0.065 **	−0.194 ***	−0.191 ***
	(0.353)	(0.284)	(1.790)	(2.068)	(−5.276)	(−5.652)
stru	0.501	0.554	0.027	−0.602	0.044	0.781
	(0.890)	(0.582)	(0.069)	(−1.257)	(0.085)	(1.196)
lnmac	−0.079	−0.085	0.221 ***	0.203 ***	−0.075	−0.073
	(−1.220)	(−1.288)	(3.164)	(2.946)	(−1.242)	(−1.310)
urban	0.280	0.265	−0.451 ***	−0.382 ***	−0.089	−0.267
	(1.034)	(0.823)	(−4.707)	(−3.163)	(−0.611)	(−1.433)
lnae	0.005	0.024	0.079	0.170 **	0.114 **	−0.001
	(0.075)	(0.160)	(1.359)	(2.185)	(2.345)	(−0.011)
ec	0.994 *	1.082 *	0.148	0.444	−0.163	0.056
	(2.033)	(1.724)	(0.538)	(1.093)	(−0.633)	(0.134)
lnrain	−0.021	−0.021	0.004	0.006	0.042 *	0.052 **
	(−0.754)	(−0.682)	(0.212)	(0.254)	(1.834)	(2.117)
cons	3.126 **	3.102 **	1.575 *	1.129	−0.939 **	−0.842 *
	(2.315)	(2.149)	(1.707)	(1.235)	(−2.102)	(−1.780)
Province-fixed effects	Yes	Yes	Yes	Yes	Yes	Yes
Time-fixed effects	No	Yes	No	Yes	No	Yes
N	620	620	620	620	620	620
R^2	0.995	0.995	0.997	0.998	0.967	0.970

Notes: The 1%, 5% and 10% levels of significance are indicated by ***, ** and *, respectively. × represents the cross-multiplication of two variables.

After controlling for time-fixed and province-fixed effects, the lagged grain direct subsidy policy has a significant inhibitory effect on carbon sinks, while its impact on GHG emissions and food security is positive but not significant. The agricultural “three subsidies” reform policy has significantly inhibited GHG emissions. The lagged policy variables have reached the same conclusion. Population density reduces the level of food security, which is related to the increased pressure on cultivated land resources and rising agricultural production costs. Agricultural disaster rates promote GHG emissions and have a negative impact on food security, indicating that reducing agricultural disaster risks, improving agricultural resilience, and adopting sustainable agricultural production methods are particularly important in addressing climate change and safeguarding food security. The improved level of agricultural mechanization has led to an increase in GHG emissions, which may be attributed to the combined effects of increased energy consumption by mechanical equipment, growth in chemical usage brought about by expanded agricultural production scale and intensification, as well as changes in land utilization methods. The urbanization rate of the population has a significant inhibitory effect on GHG emissions, while the agricultural economic development level boosts GHG emissions. The Engel coefficient has a positive impact on carbon sinks. In regions with a higher Engel coefficient, agricultural production and land use may be more focused on meeting basic food needs, further leading to more land being used for crop cultivation, thereby increasing vegetation cover and carbon sequestration capacity. Precipitation has a positive impact on food security.

3.3. Interactions among GHGs, Carbon Sinks, and Food Security

The results of the fixed effects regression indicate possible complex bidirectional causal relationships among GHG, carbon sinks, and food security. Meanwhile, the PVAR model can further capture the dynamic interactive effects among variables, which is valuable for analyzing the mutual influence of these variables across multiple time periods. In the PVAR model, all variables are assumed to be endogenous [43–46], meaning that the model inherently considers the mutual influence and dynamic relationships among variables without the need to add additional variables to "control" other potential factors that may affect the outcomes. Through the orthogonalized impulse response function, the PVAR model can directly identify the degree of impact response among different variables, revealing their interactive relationships. Subsequently, we adopt the panel vector autoregression (PVAR) model to directly focus on the dynamic causal relationships among GHGs, carbon sinks, and food security.

3.3.1. Stability Test

To avoid the issue of "false regression", we conducted a stationarity test on the panel data before estimating the PVAR model. As short panel data with Numbers = 31 and Time = 21 were used in this study, we utilized IPS and HT tests to analyze unit roots for each variable. Table 5 presents the results, which show that the variable lnGHG does not reject the null hypothesis and is non-stationary. After taking the first-order difference of all variables, another stationarity test was conducted. The results show that all variables were stationary at the 1% level, and they were consistent across PA, BA, and CA.

Table 5. Test results obtained for panel smoothness.

Variables	IPS Inspection Z-t-Tilder-Bar	*p*	HT Test z	*p*
lnfood	−8.004	0.000	−9.406	0.000
lnGHG	−0.206	0.419	0.499	0.691
lnsink	−5.980	0.000	0.280	0.610
D_lnfood	−15.228	0.000	−23.942	0.000
D_lnGHG	−12.363	0.000	−13.347	0.000
D_lnsink	−13.617	0.000	−14.036	0.000

3.3.2. GMM Estimation

Determining the optimal lag order of the model is necessary before performing PVAR analysis. The three variable sequences of lnfood, lnGHG, and lnsink were analyzed using the PVAR model. The optimal lag order was selected based on three criteria, i.e., MBIC, MAIC, and MQIC. The lag order of all areas was determined to be 1.

Based on our previous inspection and processing of variables and panel data, we constructed a PVAR model for empirical analysis using the first-order differences of all original variables as new variables. In particular, D_lnfood, D_lnGHG, and D_lnsink were used to represent the growth rates of the food security index, GHG emissions, and carbon sinks, respectively. To estimate the parameters of the model, we used the GMM with an optimal lag order of 1. The results of the model estimation are presented in Table 6. The first line displays the explained variable.

Table 6. Estimation results of GMM parameters of the PVAR model.

Variable	Area	D_lnfood	D_lnGHG	D_lnsink
L1. D_lnfood	ALL	−0.3448 ***	−0.0959	−0.3275 ***
		(0.1005)	(0.0728)	(0.1121)
	PA	−0.5040 *	−0.0040	−0.4976 **
		(0.3032)	(0.1480)	(0.2364)
	BA	−0.2368 *	−0.0866	−0.1236
		(0.0750)	(0.1087)	(0.0990)
	CA	−0.4109 ***	−0.0676	−0.3415
		(0.1412)	(0.061)	(0.2809)
L1.D_lnGHG	ALL	0.1539 *	0.0505	0.2374 **
		(0.0798)	(0.1086)	(0.0960)
	PA	0.1861	0.0153	0.2554 *
		(0.1709)	(0.1711)	(0.1487)
	BA	0.1216	0.0709	0.2414 ***
		(0.2120)	(0.1276)	(0.0880)
	CA	0.1771	0.2144	−0.0272
		(0.3911)	(0.3702)	(0.5924)
L1.D_lnsink	ALL	0.0825	0.1307 *	0.2561 **
		(0.1049)	(0.0723)	(0.1262)
	PA	0.2647	0.0554	0.2893
		(0.3788)	(0.1886)	(0.2912)
	BA	−0.1026	0.0362	−0.0499
		(0.4690)	(0.1141)	(0.1350)
	CA	0.1721	0.1335 ***	0.5234 ***
		(0.1358)	(0.0479)	(0.1869)

Notes: (1) "L1." means the lag of the first-order. (2) The 1%, 5% and 10% levels of significance are indicated by ***, ** and *, respectively. (3) The standard error values are indicated in brackets. GMM: generalized method of moments; PVAR: panel vector autoregression.

When using D_lnfood as the dependent variable, the growth rate of the food security index with a one-period lag likely has negative effects on the current year. Specifically, the whole and main grain sales areas show high significance at the 1% level, whereas the main grain production areas and BA are significant at the 10% level. Conversely, the growth rate of the warming potential with a one-period lag only has a positive impact on the growth rate of the whole food security index in the current year, but it is not significant after being classified by grain production areas. Finally, the change rate of carbon sinks in the cropland system during the previous period does not have a significant effect on food security. This finding is consistent with the regression results of the fixed effects.

When using D_lnGHG as the dependent variable, neither the change in food security nor GHG in the previous period has a significant effect on GHG in the current period. However, changes in carbon sinks during the previous period can accelerate the growth of GHG in the current period. In the fixed-effects regression results, carbon sinks can also increase GHG emissions. Notably, the main grain sales areas have the most significant effect, with significance at the 10% level throughout the entire country, but they are not significant in other regions.

When using D_lnsink as the dependent variable, the change in grain security during the previous period inhibits the growth of carbon sinks in the current period. Specifically, the effect is significant at the provincial level at 1% and major grain-producing areas show a significantly negative impact at the 5% level; however, it is not significant in other regions. Conversely, the change in GHG during the previous period can significantly promote the increase in the number of carbon sinks in the entire country, main grain production area, and balance area. The main grain sales area has a negative effect, which is not significant. Finally, the change in carbon sinks of whole agricultural systems during the previous period significantly accelerates the increase in the value of the current period, at a significant level of 5%.

To validate the robustness of our results, we conducted additional tests. Specifically, following the eigenvalue stationarity test previously proposed [45], we assessed the stability condition of the estimated PVAR model. A PVAR model is considered stable if all eigenvalues are strictly smaller than one. The results indicate that all eigenvalues are inside the unit circle at the provincial level, implying that the PVAR model satisfies the stability condition. The test results in other regions were consistent with this finding.

3.3.3. Granger Causality Test

We conducted Granger causality tests using the PVAR model. The test comprises two hypotheses, namely H0, which excluded variable does not Granger-cause Equation, and Ha, which excluded variable Granger-causes Equation [45]. The original hypothesis of the absence of causality was rejected for the variable sequences at the 1%, 5%, and 10% significance levels (Table 7). Specifically, the change in GHG at the provincial level was determined to be mutually causal with the changes in the food security index and carbon sinks. Furthermore, the changes in the food security index were identified as the reasons for variation in carbon sinks. The changes in the food security index and GHG of major grain-producing areas were identified as Granger factors of carbon sinks changes. Additionally, the GHG of the grain balance area was determined to be the Granger cause of carbon sinks changes. In contrast, the carbon sinks changes of the main grain sales area were identified as the Granger cause of GHG changes.

Table 7. Granger causality test results.

Equation	**Excluded**	**All**			**PA**			**BA**			**CA**		
		chi^2	**df**	***p***	**chi^2**	**df**	***p***	**chi^2**	**df**	***p***	**chi^2**	**df**	***p***
D_lnfood	D_lnGHG	3.713	1	0.054	1.186	1	0.276	1.557	1	0.212	0.205	1	0.651
	D_lnsink	0.618	1	0.432	0.488	1	0.485	0.524	1	0.469	1.605	1	0.205
	ALL	4.405	2	0.111	3.580	2	0.167	1.660	2	0.436	1.741	2	0.419
D_lnGHG	D_lnfood	1.732	1	0.188	0.001	1	0.978	0.635	1	0.426	1.226	1	0.268
	D_lnsink	3.264	1	0.071	0.086	1	0.769	0.101	1	0.751	7.778	1	0.005
	ALL	4.426	2	0.109	1.566	2	0.457	1.180	2	0.554	7.975	2	0.019
D_lnsink	D_lnfood	8.533	1	0.003	4.430	1	0.035	1.560	1	0.212	1.478	1	0.224
	D_lnGHG	6.111	1	0.013	2.949	1	0.086	7.522	1	0.006	0.002	1	0.963
	ALL	11.026	2	0.004	12.963	2	0.002	8.025	2	0.018	1.579	2	0.454

3.3.4. Impulse Response Function (IRF)

The IRF reveals how variables react when subjected to a shock or innovation in other variables, and provides information regarding the duration required for the series to return to a stable state [47]. In this study, we utilized 200 Monte Carlo simulations based on a Gaussian approximation to estimate the confidence intervals for IRF using Cholesky decomposition [45]. Since not all variables in all regions exhibited Granger causality, impulse response analysis was only conducted on variables with Granger causality (Figure 4).

When the carbon sink is affected by one standard deviation, a strong positive response is observed in the carbon sinks of the whole country and each region, followed by a rapid decrease (Figure 4a–c). However, this effect disappears after the fourth period. The D_lnGHG in all areas and in major grain sales areas exhibits the maximum positive response in the first period, followed by a sharp decline, and gradually s to zero after the fourth period. The pulse effect of D_lnfood is not significant in all regions.

When the GHG is affected by one standard deviation, the impulse responses of D_lnsink in the whole country, main grain production area, and balance area are positive, reaching the maximum and minimum values in the first and second period, respectively. They gradually converge to zero (Figure 4d–f). Except for the GHG in the main grain sales area, which exhibits no significant response, the positive response of the GHG itself decreases rapidly in the first period and starts to gradually converge to zero in the second period. The responses of D_lnfood and D_lnsink in all areas are consistent, but D_lnfood exhibits a negative response in the second period and tends to be stable after the fourth period. The pulse effect of D_lnfood in other regions is not significant.

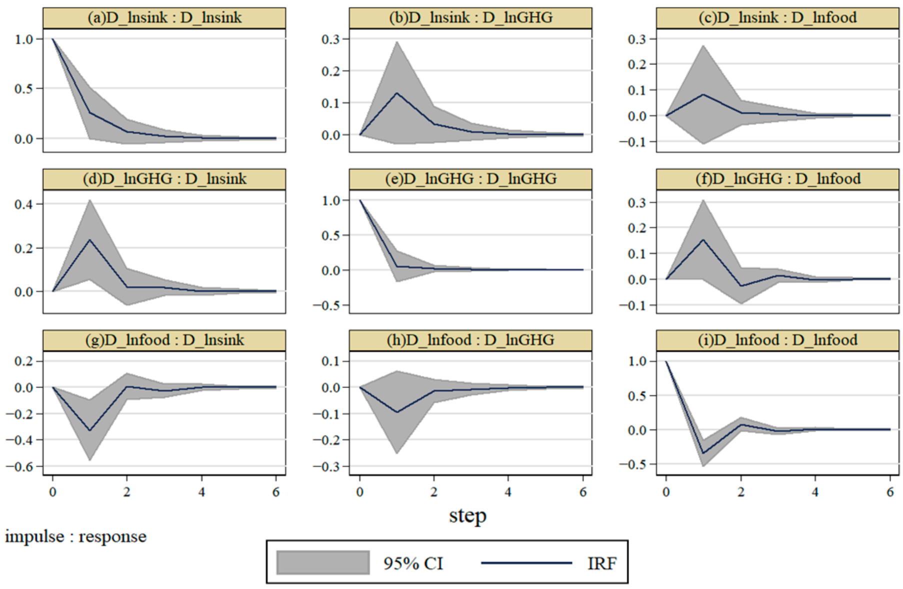

Figure 4. Graphs of orthogonalized IRFs.

When food security is affected by one standard deviation, the impulse response of D_lnsink in the whole country and major grain-producing areas is negative, reaching the minimum value in the first period, and gradually converging to zero in the fourth period (Figure 4g–i). The impulse response of D_lnGHG is not significant in all regions. In all regions, the impulse response of D_lnfood first exhibits a positive and then a negative trend, reaching the minimum value in the first period. The response decline speed is significantly greater than that of D_lnsink and tends to stabilize after the fourth period.

3.3.5. Variance Decomposition

Based on the variance decomposition results, the following observations can be made. First, the food security index in all regions are primarily influenced by their past values. Starting from the second period, the GHG has a weak effect (<3%) on food security. This effect stabilizes in the fourth period. Second, the GHG of all regions is mostly driven by its past values and remains stable up to the fourth lag period. The contribution of food security to the GHG varies from high to low across different regions, with PA (4.68%), BA (4.04%), All regions (3%), and CA (2.85%) having the highest to lowest contributions, respectively. In CA, carbon sinks have the most significant effect on the GHG, reaching 5.56% in the sixth period. Finally, except for CA, food security affects > 50% of the carbon sinks in all other regions. The impact on carbon sinks reaches 92.18% in major grain-producing areas. Carbon sinks in the main grain sales area are primarily affected by past values, reaching a maximum value of 45.97% in the sixth period. The GHG contributes the least to the carbon sink.

4. Discussion

4.1. Non-CO_2 Greenhouse Gases from Agricultural Systems

Carbon emissions, among the main GHG emissions, have received considerable attention [48]. The agricultural system has dual functions (carbon emissions and carbon sinks), making it an important contributor to global emission reduction and sink increase. However, non-CO_2 greenhouse gases, including CH_4 and N_2O with high warming potential [49], are often overlooked in agricultural production activities [50], resulting in the greenhouse effect of the cropland system being underestimated. According to reports, the annual increase in CH_4 concentration from 2020 to 2021 was the highest on record [51]. The GHG emissions from paddy fields are more than four times those of wheat, which is primarily driven by CH_4 and not N_2O [52,53]. The results of our study showed that, after the uniform warming potential conversion, the warming potential due to CH_4 and N_2O emissions from agricultural systems is much higher than that of CO_2. Strengthening regulatory mechanisms is recommended to ensure comprehensive consideration of CH_4 and N_2O emissions when assessing the greenhouse effect of agricultural systems. As the ratio of N fertilizer application in China's agriculture has decreased, the emissions of N_2O have also declined. However, CH_4 mainly comes from paddy field production activities, and emissions have slightly decreased since 2018 due to changes in the planting structure and adjustment of the sowing area. Paddy fields are also important carbon sinks, and the correlation results show that CH_4 emissions and carbon sinks significantly correlate in all regions. Paddy fields are a major staple food crop, the methane emissions of which must not be ignored as they have significant implications for global climate change. Nevertheless, high rice yields do not necessarily equate to high emissions [54]. Through improvements in rice varieties and cultivation practices, achieving sustainable food production with high yields and low emissions remains a viable possibility. These improvements should focus on adjusting the planting and fertilization structure of rice paddies, which could be achieved using direct-seeding rice instead of seedling transplantation, using cover materials, raising water levels to reduce the use of nitrogen and chemical fertilizers, promoting the use of efficient microbial agents to inhibit methane-generating bacteria in rice paddies, and increasing the biodiversity of the rice paddy ecosystem to reduce methane emissions. Moreover, the establishment of a monitoring system is crucial to regularly assess the effectiveness of rice paddy ecosystem management, allowing for adjustments and improvements based on actual conditions.

4.2. Effect of Agricultural Policies on GHGs, Carbon Sinks, and Food Security

The effect of China's agricultural policies implemented at different stages on GHGs, carbon sinks, and food security revealed that the direct grain subsidy policy has not achieved the policy objective of ensuring food security, consistent with the findings by Zang et al. [55]. On the contrary, the one-period lagged direct grain subsidy policy has reduced carbon sinks in the agricultural system. The grain direct subsidy policy, which has been fully implemented since 2004, aims to encourage increased planting areas and improved grain yields, prompting farmers to use additional fertilizers, pesticides, and other agricultural inputs. However, this subsidy approach may cause farmers to expand grain-growing areas through over-exploitation of land, thereby destroying the original vegetation cover and reducing the carbon sink capacity of the ecosystem. Notably, the agricultural "three subsidies" reform policy has not directly promoted food security, which may be due to shortcomings in the design or implementation of the policy. However, this policy has played a significant role in suppressing GHG emissions. The policy measures implemented in the previous year had the same effect. This is related to the adjustment of the policy objectives to support the protection of soil fertility and the moderate scale operation of grain production, indicating that the implementation of this policy is conducive to emission reduction and carbon sequestration in the agricultural system. Although we identified the role of the nationwide grain direct subsidy policy in GHGs, carbon sinks, and food security by controlling provincial, time-fixed effects, as well as the interaction effects between provinces and time, we did not consider the differences in subsidy methods and amounts of grain direct subsidies in different regions owing to the availability of data and the focus of this study. Consequently, our assessment of policy effects may be biased and may prevent us from fully reflecting the actual role of the policy in promoting agricultural sustainable development and ensuring food security. To achieve a more precise evaluation of policy impacts, future research studies should aim to gather and enhance pertinent data, considering the multifaceted influences of regional disparities, varying subsidy methodologies, and diverse subsidy amounts.

4.3. The Relationship among GHGs, Carbon Sinks, and Food Security

The results of previous research indicated a two-way correlation between China's agricultural output and GHG emissions [28]. However, in contrast to China, no causal relationship has been identified between Japan's agricultural output and carbon emissions, although any imbalances between the two are likely to require approximately 116 years to achieve long-term sustainability [56]. The results of our study show that there is only a one-way correlation between food security and GHG emissions. From the perspective of the long-term warming potential, an increase in food security capacity will not directly lead to the aggravation of the greenhouse effect. In contrast, the warming potential of GHG in agricultural systems has a "fertilization effect" on crops at the provincial level. Unfortunately, changes in the food security index can easily reduce carbon sinks rate of agricultural systems, which may be related to problems such as soil compaction and acidification caused by the long-term excessive application of chemical fertilizers, consistent with Zhang et al. [57]. This can weaken the soil's carbon sink capacity. According to Wang et al. [12], an increase in atmospheric CO_2 concentration enhances the carbon sink capacity of terrestrial ecosystems. We have reached the same conclusion in the field of agriculture, which is an increase in carbon sinks in agricultural systems at the whole level also contributes to the increase in the warming potential (Figure 5); however, the warming potential can also have indirect adverse effects on carbon sinks by promoting food security. Therefore, when formulating agricultural policies and strategies, it is essential to integrate agricultural emission reduction and carbon sinks with food security within the same framework. It is also important to globally recognize the significance of this comprehensive approach in simultaneously promoting sustainable agriculture and ensuring global food security. The focus should be on addressing the conflicts among these three factors.

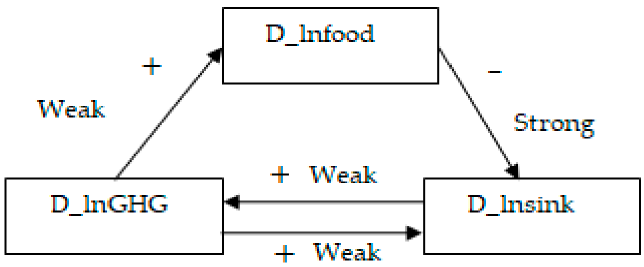

Figure 5. Diagrammatic representation of the relationship among GHGs, carbon sinks, and food security.

The conflict relationships among GHGs, carbon sinks, and food security varies across different grain functional zones, necessitating regional classification for targeted measures. In terms of different zones, except for CA, the warming potential of GHG in agricultural systems increases the carbon sink capacity of crops, and simultaneously, the carbon sink capacity will increase GHG emissions in the next period. Proper handling of the relationship between the two is key to making full use of agricultural systems to reduce emissions and increase sinks. In addition, our research shows that excessively pursuing the rapid growth of the food security index will put pressure on food security in the next year. Excessive emphasis on food security, particularly the increase in grain production, may lead to inadequate resource allocation and alter land-use patterns, exerting significant pressure on PA. This affects the sustainability of agricultural systems and, consequently, has adverse implications for future food security. To alleviate this, it is advisable to consider local economic conditions and resource-carrying capacity thoroughly when formulating food security standards. Due to variations in the interactions among food security, GHGs, and carbon sinks in different regions, we recommend establishing demonstration zones for agricultural emission reduction and carbon sinks based on representative regions classified according to different grain functional zones, rather than implementing a uniform policy across all regions. PAs are responsible for food production and should focus on promoting sustainable land-use practices such as crop rotation, conservation tillage, and the use of cover crops. The promotion of low-carbon technologies can also reduce the negative effect of food security on carbon sinks growth. Considering the income of grain farmers, it is recommended to pilot agricultural carbon markets where grain farmers can sell carbon sinks to obtain corresponding economic benefits, thereby encouraging the implementation of independent emission reduction measures. This can promote sustainable agricultural practices and efficient resource utilization, ensuring the sustainable production of food. BA, such as Gansu and Shaanxi provinces, located in the food balance area, are typical arid and semi-arid regions in which heat-, drought-, and pest-resistant varieties can be promoted. These varieties can also make full use of the increased GHG emissions to promote carbon sinks. In CA, the focus should be placed on measures to reduce GHG emissions, such as the use of clean energy, improving energy efficiency, promoting organic agriculture, and the modernization of farmland water conservancy projects.

4.4. Limitations

This article provides a comprehensive analysis of the interactive dynamics among GHG emissions reduction, carbon sinks and food security in the agricultural system. However, it has yet to delve into the factors that underlie the formation of such interactions. Furthermore, various nations have introduced a multitude of policy measures to curtail carbon emissions but are also confronted with challenges concerning food security. If we can anticipate the trends in GHG emissions, carbon sinks, and food security under different policy scenarios in the future, this research could facilitate policy adjustments to foster a harmonious and mutually beneficial relationship among the three components.

5. Conclusions

This study examined trends in GHGs, carbon sinks, and food security in China's agricultural systems from 2000 to 2020, using panel data from 31 provinces. Granger causality tests, the PVAR model, and impulse responses were employed to analyze their interaction. The key findings are as follows:

First, from 2001 to 2020, food security and carbon sinks increased overall, and GHGs began declining after 2016. The PA had the highest mean GHGs, followed by CA, and then BA, which had the lowest. Carbon sinks and food security ranked highest in PA, followed by BA and then CA. Some provinces, like Hebei, Jiangsu, Shandong, and Sichuan, showed improved GHGs reduction, carbon sinks, and food security in PA, while others, like Shanxi, Guangxi, and Chongqing showed these improvements in the BA, and Tianjin in the CA.

Second, CH_4 emissions contribute most to the warming potential, while CO_2 contributes the least. When evaluating the greenhouse effect, more attention should be placed on reducing CH_4 and N_2O emissions rather than on CO_2 alone. While a significant overall correlation exists among GHGs, carbon sinks, and food security, at the grain functional zones level, sinks–GHGs correlate in all regions, sinks–food security significantly correlate in PA and BA, and GHGs–food security correlate weakly in BA and CA.

Finally, when integrating GHGs, carbon sinks, and food security into the same system, changes in GHGs and carbon sinks exhibit good self-coordination, but changes in food security has short-term positive and long-term negative effects on food security itself. Multiple conflicting correlations exist among the three factors. Overall, carbon changes positively affect a rise in GHGs, but food security strongly inhibits carbon sink increases. In the grain functional zones, GHG changes positively affect carbon sinks in BA, while food security negatively impacts carbon sinks (up to 90%) in PA.

Author Contributions: W.Y.: Conceptualization, Methodology, Investigation, Writing—original draft, Visualization, Software. X.M.: review & editing. All authors have read and agreed to the published version of the manuscript.

Funding: This research was funded by Philosophy and Social Science Foundation of Hunan Province (Grant No.: 23YBQ137), Scientific Research Fund of Hunan Provincial Education Department, China (Grant No.: 23B0884, 19A081).

Institutional Review Board Statement: Not applicable.

Data Availability Statement: The data presented in this study are available upon request from the corresponding author.

Conflicts of Interest: The authors declare no conflicts of interest.

References

1. Balwinder, S.; Shirsath, P.B.; Jat, M.L.; McDonald, A.J.; Srivastava, A.K.; Craufurd, P.; Rana, D.S.; Singh, A.K.; Chaudhari, S.K.; Sharma, P.C.; et al. Agricultural labor, COVID-19, and potential implications for food security and air quality in the breadbasket of India. *Agric. Syst.* **2020**, *185*, 102954. [CrossRef]
2. Mauricio Galeana-Pizana, J.; Couturier, S.; Figueroa, D.; Daniel Jimenez, A. Is rural food security primarily associated with smallholder agriculture or with commercial agriculture?: An approach to the case of Mexico using structural equation modeling. *Agric. Syst.* **2021**, *190*, 103091. [CrossRef]
3. Song, S.; Goh, J.C.L.; Tan, H.T.W. Is food security an illusion for cities? A system dynamics approach to assess disturbance in the urban food supply chain during pandemics. *Agric. Syst.* **2021**, *189*, 103045. [CrossRef]
4. Food and Agriculture Organization (FAO). *The State of the World's Land and Water Resources for Food and Agriculture–Systems at Breaking Point*; Food and Agriculture Organization: Rome, Italy, 2021.
5. Luo, Y.; Long, X.; Wu, C.; Zhang, J. Decoupling CO_2 emissions from economic growth in agricultural sector across 30 Chinese provinces from 1997 to 2014. *J. Clean. Prod.* **2017**, *159*, 220–228. [CrossRef]
6. Olayide, O.E.; Tetteh, I.K.; Popoola, L. Differential impacts of rainfall and irrigation on agricultural production in Nigeria: Any lessons for climate-smart agriculture? *Agric. Water Manag.* **2016**, *178*, 30–36. [CrossRef]
7. Thiault, L.; Mora, C.; Cinner, J.E.; Cheung, W.W.L.; Graham, N.A.J.; Januchowski-Hartley, F.A.; Mouillot, D.; Sumaila, U.R.; Claudet, J. Escaping the perfect storm of simultaneous climate change impacts on agriculture and marine fisheries. *Sci. Adv.* **2019**, *5*, eaaw9976. [CrossRef]
8. Frank, S.; Havlík, P.; Soussana, J.-F.; Levesque, A.; Valin, H.; Wollenberg, E.; Kleinwechter, U.; Fricko, O.; Gusti, M.; Herrero, M.; et al. Reducing greenhouse gas emissions in agriculture without compromising food security? *Environ. Res. Lett.* **2017**, *12*, 105004. [CrossRef]
9. Smith, P.; Haberl, H.; Popp, A.; Erb, K.H.; Lauk, C.; Harper, R.; Tubiello, F.N.; de Siqueira Pinto, A.; Jafari, M.; Sohi, S.; et al. How much land-based greenhouse gas mitigation can be achieved without compromising food security and environmental goals? *Glob. Chang. Biol.* **2013**, *19*, 2285–2302. [CrossRef]
10. Hasegawa, T.; Fujimori, S.; Shin, Y.; Tanaka, A.; Takahashi, K.; Masui, T. Consequence of climate mitigation on the risk of hunger. *Environ. Sci. Technol.* **2015**, *49*, 7245–7253. [CrossRef]
11. Herrero, M.; Henderson, B.; Havlík, P.; Thornton, P.K.; Conant, R.T.; Smith, P.; Wirsenius, S.; Hristov, A.N.; Gerber, P.; Gill, M.; et al. Greenhouse gas mitigation potentials in the livestock sector. *Nat. Clim. Chang.* **2016**, *6*, 452–461. [CrossRef]
12. Wang, S.; Zhang, Y.; Ju, W.; Chen, J.; Peuelas, J. Recent global decline of CO_2 fertilization effects on vegetation photosynthesis. *Science* **2020**, *370*, 1295–1300. [CrossRef] [PubMed]
13. Lobell, D.B.; Field, C.B. Estimation of the carbon dioxide (CO_2) fertilization effect using growth rate anomalies of CO_2 and crop yields since 1961. *Glob. Chang. Biol.* **2008**, *14*, 39–45. [CrossRef]
14. Bloom, A.J.; Burger, M.; Kimball, B.A.; Pinter, J.P.J. Nitrate assimilation is inhibited by elevated CO_2 in field-grown wheat. *Nat. Clim. Chang.* **2014**, *4*, 477–480. [CrossRef]
15. Myers, S.S.; Zanobetti, A.; Kloog, I.; Huybers, P.; Leakey, A.D.; Bloom, A.J.; Carlisle, E.; Dietterich, L.H.; Fitzgerald, G.; Hasegawa, T.; et al. Increasing CO_2 threatens human nutrition. *Nature* **2014**, *510*, 139–142. [CrossRef] [PubMed]
16. Tang, X.; Zhao, X.; Bai, Y.; Tang, Z.; Wang, W.; Zhao, Y.; Wan, H.; Xie, Z.; Shi, X.; Wu, B.; et al. Carbon pools in China's terrestrial ecosystems: New estimates based on an intensive field survey. *Proc. Natl. Acad. Sci. USA* **2018**, *115*, 4021–4026. [CrossRef]
17. Lal, R. Soil carbon sequestration impacts on global climate change and food security. *Science* **2004**, *304*, 1623–1627. [CrossRef] [PubMed]
18. Zhou, W.; Long, W.; Wang, H.; Long, P.; Xu, Y.; Zhong, K.; Xiong, R.; Xie, F.; Chen, F.; Fu, Z. Reducing carbon footprints and increasing net ecosystem economic benefits through dense planting with less nitrogen in double-cropping rice systems. *Sci. Total Environ.* **2023**, *891*, 164756. [CrossRef] [PubMed]
19. Piao, S.; Sitch, S.; Ciais, P.; Friedlingstein, P.; Peylin, P.; Wang, X.; Ahlstrom, A.; Anav, A.; Canadell, J.G.; Cong, N.; et al. Evaluation of terrestrial carbon cycle models for their response to climate variability and to CO_2 trends. *Glob. Change Biol.* **2013**, *19*, 2117–2132. [CrossRef]

20. Schimel, D.; Stephens, B.B.; Fisher, J.B. Effect of increasing CO_2 on the terrestrial carbon cycle. *Proc. Natl. Acad. Sci. USA* **2015**, *112*, 436–441. [CrossRef] [PubMed]
21. Keenan, T.F.; Luo, X.; De Kauwe, M.G.; Medlyn, B.E.; Prentice, I.C.; Stocker, B.D.; Smith, N.G.; Terrer, C.; Wang, H.; Zhang, Y.; et al. Retraction Note: A constraint on historic growth in global photosynthesis due to increasing CO_2. *Nature* **2022**, *606*, 420. [CrossRef]
22. Terrer, C.; Jackson, R.B.; Prentice, I.C.; Keenan, T.F.; Kaiser, C.; Vicca, S.; Fisher, J.B.; Reich, P.B.; Stocker, B.D.; Hungate, B.A.; et al. Nitrogen and phosphorus constrain the CO_2 fertilization of global plant biomass. *Nat. Clim. Chang.* **2019**, *9*, 684–689. [CrossRef]
23. Winkler, A.J.; Myneni, R.B.; Hannart, A.; Sitch, S.; Haverd, V.; Lombardozzi, D.; Arora, V.K.; Pongratz, J.; Nabel, J.E.M.S.; Goll, D.S.; et al. Slowdown of the greening trend in natural vegetation with further rise in atmospheric CO_2. *Biogeosciences* **2021**, *18*, 4985–5010. [CrossRef]
24. Ashraf, J.; Javed, A. Food security and environmental degradation: Do institutional quality and human capital make a difference? *J. Environ. Manag.* **2023**, *331*, 117330. [CrossRef] [PubMed]
25. Sarker, A. Ecological perspectives on water, food, and health security linkages: The Minamata case in Japan. *Environ. Sci. Pollut. Res.* **2021**, *28*, 32177–32189. [CrossRef] [PubMed]
26. Fan, D.; Fan, Y.; Tian, Z.; Li, X.; Jiang, M.; Sun, L.; Zhong, H.; Wang, K.; Wang, X.; Jiang, L. A vital option for food security and greenhouse gases mitigation: Planting elite super rice in double- to single-rice cropping fields in China. *Environ. Res. Lett.* **2021**, *16*, 094038. [CrossRef]
27. Fujimori, S.; Wu, W.; Doelman, J.; Frank, S.; Hristov, J.; Kyle, P.; Sands, R.; van Zeist, W.J.; Havlik, P.; Dominguez, I.P.; et al. Land-based climate change mitigation measures can affect agricultural markets and food security. *Nat. Food* **2022**, *3*, 110–121. [CrossRef] [PubMed]
28. Al-mulali, U.; Fereidouni, H.G.; Bin Mohammed, M.A.H.; Lee, J.Y.M. Agriculture investment, output growth, and CO2emissions relationship. *Energy Sources Part B Econ. Plan. Policy* **2016**, *11*, 665–671. [CrossRef]
29. Cheng, P.; Tang, H.; Lin, F.; Kong, X. Bibliometrics of the nexus between food security and carbon emissions: Hotspots and trends. *Environ. Sci. Pollut. Res. Int.* **2023**, *30*, 25981–25998. [CrossRef] [PubMed]
30. Liu, D.D.; Zhu, X.Y.; Wang, Y.F. China's agricultural green total factor productivity based on carbon emission: An analysis of evolution trend and influencing factors. *J. Clean. Prod.* **2021**, *278*, 123692. [CrossRef]
31. Inubushi, K.; Cheng, W.G.; Aonuma, S.; Hoque, M.M.; Kobayashi, K.; Miura, S.; Kim, H.Y.; Okada, M. Effects of free-air CO_2 enrichment (FACE) on CH_4 emission from a rice paddy field. *Glob. Chang. Biol.* **2003**, *9*, 1458–1464. [CrossRef]
32. Intergovernmental Panel on Climate Change (IPCC). *Climate Change 2007: The Physical Science Basis*; Cambridge University Press: Cambridge, UK, 2007.
33. Min, J.; Hu, H. Calculation of Greenhouse Gases Emission from Agricultural Production in China. *China Popul. Resour. Environ.* **2012**, *22*, 21–27. (In Chinese)
34. Huang, X.; Xu, X.; Wang, Q.; Zhang, L.; Gao, X.; Chen, L. Assessment of Agricultural Carbon Emissions and Their Spatiotemporal Changes in China, 1997-2016. *Int. J. Environ. Res. Public Health* **2019**, *16*, 3105. [CrossRef]
35. Yue, Q.; Wu, H.; Sun, J.F.; Cheng, K.; Smith, P.; Hillier, J.; Xu, X.R.; Pan, G.X. Deriving Emission Factors and Estimating Direct Nitrous Oxide Emissions for Crop Cultivation in China. *Environ. Sci. Technol.* **2019**, *53*, 10246–10257. [CrossRef] [PubMed]
36. Tian, H.; Xu, R.; Canadell, J.G.; Thompson, R.L.; Winiwarter, W.; Suntharalingam, P.; Davidson, E.A.; Ciais, P.; Jackson, R.B.; Janssens-Maenhout, G.; et al. A comprehensive quantification of global nitrous oxide sources and sinks. *Nature* **2020**, *586*, 248–256. [CrossRef] [PubMed]
37. Xu, S.; Liu, J.; Wang, Y.; Zheng, N. Variation characteristics analysis of major crop carbon fixation in SanjiangPlain during 1980~2007. *J. Arid Land Resour. Environ.* **2011**, *25*, 179–183.
38. Zhang, M.; Chen, Y.; Yu, C.; Pan, Z.; Fan, D.; Luo, Y.; Wang, X. Dynamic assessments of plant biomass and carbon storage during the production cycle of tea gardens. *J. Zhejiang Univ.* **2013**, *39*, 687–694. (In Chinese) [CrossRef]
39. Li, K. *Land Use Change and Net Greenhouse Gas Emissions and Terrestrial Ecosystem Carbon Cycle*; China Meteorological Press: Beijing, China, 2002. (In Chinese)
40. Johnson, J.D.; Allmaras, D.; Reicosky, R. Estimating source carbon residues, roots and rhizodeposits using the nation grain-yield database. *Agron. J.* **2006**, *98*, 622–636. [CrossRef]
41. Shi, P.; Feng, Z.H.; Gao, H.D.; Li, P.; Zhang, X.M.; Zhu, T.; Li, Z.B.; Xu, G.C.; Ren, Z.P.; Xiao, L. Has "Grain for Green" threaten food security on the Loess Plateau of China? *Ecosyst. Health Sustain.* **2020**, *6*, 1709560. [CrossRef]
42. Cai, Y.; Fu, Z.; Dai, E. The minimum area per capita of cultivated land and its implication for the optimization of land resource allocation. *Acta Geogr. Sin.* **2002**, *57*, 127–134. (In Chinese)
43. Holtz-Eakin, D.; Newey, W.; Rosen, H.S. Estimating Vector Autoregressions with Panel Data. *Econometrica* **1988**, *56*, 1371–1395. [CrossRef]
44. Shao, Q.; Liu, X.; Zhao, W. An alternative method for analyzing dimensional interactions of urban carrying capacity: Case study of Guangdong-Hong Kong-Macao Greater Bay Area. *J. Environ. Manag.* **2020**, *273*, 111064. [CrossRef] [PubMed]
45. Abrigo, M.R.M.; Love, I. Estimation of panel vector autoregression in Stata. *Stata J.* **2016**, *16*, 778–804. [CrossRef]
46. Bakirtas, I.; Cetin, M.A. Revisiting the environmental Kuznets curve and pollution haven hypotheses: MIKTA sample. *Environ. Sci. Pollut. Res.* **2017**, *24*, 18273–18283. [CrossRef] [PubMed]
47. Kumeka, T.T.; Uzoma-Nwosu, D.C.; David-Wayas, M.O. The effects of COVID-19 on the interrelationship among oil prices, stock prices and exchange rates in selected oil exporting economies. *Resour. Policy* **2022**, *77*, 102744. [CrossRef] [PubMed]

48. Andreoni, V.; Duriavig, M. The responsibility of CO_2 embodied in Italy–China trade: A consumption-based approach. *Int. J. Sustain. Econ.* **2011**, *3*, 44–62.
49. Yan, C.; Han, M.; Liu, Y.; Zhang, B. Household CH_4 and N_2O Footprints of Major Economies. *Earths Future* **2021**, *9*, e2021EF002143. [CrossRef]
50. Li, D. Analysis of Agricultural Biomass Energy Use and Greenhouse Gas Reduction Evidence from China. *J. Environ. Public Health* **2022**, *2022*, 6126944. [CrossRef] [PubMed]
51. World Meteorological Organization (WMO). *State of the Global Climate 2022*; World Meteorological Organization: Geneva, Switzerland, 2023.
52. Linquist, B.; Groenigen, K.J.; Adviento-Borbe, M.A.; Pittelkow, C.; Kessel, C. An agronomic assessment of greenhouse gas emissions from major cereal crops. *Glob. Chang. Biol.* **2012**, *18*, 194–209. [CrossRef]
53. Pathak, H.; Jain, N.; Bhatia, A.; Patel, J.; Aggarwal, P.K. Carbon footprints of Indian food items. *Agriculture, Ecosyst. Environ.* **2010**, *139*, 66–73. [CrossRef]
54. Su, J.; Hu, C.; Yan, X.; Jin, Y.; Chen, Z.; Guan, Q.; Wang, Y.; Zhong, D.; Jansson, C.; Wang, F.; et al. Expression of barley SUSIBA2 transcription factor yields high-starch low-methane rice. *Nature* **2015**, *523*, 602–606. [CrossRef]
55. Zang, W.R.; Fu, X.H.; Xiong, D.P. The effect evaluation of direct financial subsidy policy on the food amount security. *J. Agrotech. Econ.* **2010**, *12*, 84–93. (In Chinese)
56. Ratnatunga, J.; Murad, M.W. Carbonomics of Japan's agricultural output: Causality and long-run sustainability. *Int. J. Sustain. Dev. World Ecol.* **2012**, *19*, 482–489. [CrossRef]
57. Zhang, J.; Tian, H.; Shi, H.; Zhang, J.; Wang, X.; Pan, S.; Yang, J. Increased greenhouse gas emissions intensity of major croplands in China: Implications for food security and climate change mitigation. *Glob. Chang. Biol.* **2020**, *26*, 6116–6133. [CrossRef] [PubMed]